AIAA JOURNAL
Vol. 32, No. 3, March 1994

Buckling Analysis of Laminated Cylindrical Shells with Arbitrary Noncircular Cross Section

Izhak Sheinman* and Marina Firer†
Technion—Israel Institute of Technology, Haifa, Israel

Buckling analysis of laminated cylindrical shells with noncircular cross section of arbitrary closed shape is presented. The equations, in terms of the normal displacement and Airy stress function, of the Donnell type, are derived via the Hu-Washizu mixed formulation. The curvature, which is a function of the circumferential coordinate, is expanded in Fourier series. The circumferential dependence is eliminated by a combination of Fourier expansion and Galerkin's method. The resulting ordinary differential equations are then reduced to matrix equations by the use of finite differences. The configurational aspect is investigated parametrically. Unlike the circular cylindrical shells, coupling of the wave number in the circumferential direction is significantly high.

I. Introduction

THE advent of laminate composite materials opened the way for efficient shell structures with arbitrary cross section. Shells with a noncircular cross section are already widely used in industrial applications. Their buckling and postbuckling behavior is a vital safety consideration. Thus, improvements in the accuracies of predicting this behavior are essential for reliable design.

The nonlinear behavior of shell-like structures is generally characterized by a limit point rather than by a bifurcation point (buckling analysis); still, bifurcation analysis can be used as a guideline and a basic procedure for examining the imperfection sensitivity.

Although numerous research works on the buckling and postbuckling behavior of shells with circular cross sections have appeared over the last 80 years (see Ref. 1), literature on noncircular cross sections is very scanty. A review of the earliest works can be found in Volpe et al.[2,3] These include the papers of Kempner and Chen[4,5] and later those of Hutchinson,[6] Feinstein et al.,[7,8] and Chen and Kempner.[9] Buckling of laminated composite noncircular cylindrical shells was analyzed by Soldatos and Tzivanidis[10] and more recently by Sun.[11] All of these papers deal with specific noncircular shapes, namely, elliptic and oval ones, whose relative imperfection sensitivity was studied by Hutchinson.[6]

The object of the present work is a refined buckling analysis for laminated cylindrical shells with a noncircular cross section of arbitrary closed shape. The closed shape may be treated as a periodic function and accordingly expanded in Fourier series in terms of the circumferential angle coordinate.

Of the different shell theories,[2,12,13] Donnell-type equations were adopted here for the kinematic approach because of their relative simplicity. They are sufficiently accurate, provided both the length of the cylinder and the oval eccentricity parameter are small. For larger values, they can be used only for indication of the behavior. The analysis is based on the classical laminate theory, and the equations are written in terms of the normal displacement W and the Airy stress function F. The solution procedure is based on separation of the variables as Fourier series in the circumferential direction and by finite differences in the meridional direction. Since the curvature is written, for convenience, in terms of circumferential angle coordinate θ rather than in terms of the circumferential arc length, the system is transformed to the former. The Galerkin procedure is used to minimize the errors due to the truncated series and the noncompliance of the boundary conditions. The procedure is illustrated on an isotropic and laminated noncircular cylindrical shell under axial compression. The configuration aspect is examined parametrically in the elliptic and oval cross-sectional cases.

II. Mathematical Formulation and Geometry of Noncircular Cylinder

Let (x, y) be the shell coordinates of the reference surface and z the inward normal coordinate (Fig. 1). Application of the Kirchhoff-Love hypothesis as basic assumption leaves three dependent variables U, V, and W, respectively. Resorting to the von Kármán nonlinear kinematic approach for a perfect shell, one can write the strain displacement as

$$\{\epsilon\} = \{\bar{\epsilon}\} + z\{\chi\} \tag{1}$$

where

$$\{\bar{\epsilon}\} = \begin{Bmatrix} U_{,x} + \tfrac{1}{2}W_{,x}^2 \\ W_{,y} - \dfrac{W}{R(\theta)} + \tfrac{1}{2}W_{,y}^2 \\ U_{,y} + V_{,x} + W_{,x}W_{,y} \end{Bmatrix}$$

$$\{\chi\} = \begin{Bmatrix} -W_{,xx} \\ -W_{,yy} \\ -2W_{,xy} \end{Bmatrix} \tag{2}$$

where $(\,)_{,x}$ and $(\,)_{,y}$ denote the derivatives in the meridional x and circumferential y directions, respectively.

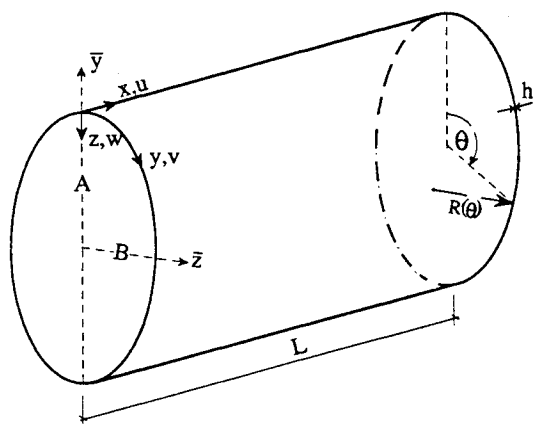

Fig. 1 Geometry and sign convention for coordinates and displacements.

Received March 1, 1993; revision received June 28, 1993; accepted for publication June 30, 1993.

*Professor, Department of Civil Engineering.
†Graduate Student, Department of Civil Engineering.

Introduction of the Airy stress function F reduces the system to only two dependent variables W and F. The function is defined by the following relationship:

$$\{N\} = \{F\} + \{\bar{N}\} \tag{3}$$

where $\{N\}^T = \{N_{xx}, N_{yy}, N_{xy}\}$ is the internal membrane force vector, $\{\hat{F}\} = \{F_{,yy}, F_{,xx}, -F_{,xy}\}$ the Airy stress vector, and $\{\bar{N}\}^T = \{\bar{N}_{xx}, \bar{N}_{yy}, \bar{N}_{xy}\}$ the external in-plane loading applied at the boundaries.

Under the classical laminate theory the strain $\{\bar{\varepsilon}\}$ and the bending moment $\{M\}^T$ $(= \{M_{xx}, M_{yy}, M_{xy}\})$ can be expressed in terms of $\{\hat{F}\}$, the curvature $\{\chi\}$, and the in-plane external loading $\{\bar{N}\}$ as

$$\begin{aligned} \{\bar{\varepsilon}\} &= [a]\{\hat{F} + \bar{N}\} - [b]\{\chi\} \\ \{M\} &= [b]^T\{\hat{F} + \bar{N}\} + [d]\{\chi\} \end{aligned} \tag{4}$$

where $a = A^{-1}$, $b = A^{-1}B$, $d = D - BA^{-1}B$,

$$(A_{ij}, B_{ij}, D_{ij}) = \int_Z Q_{ij}(1, z, z^2)\, dz \tag{5}$$

where A_{ij}, B_{ij}, and D_{ij} are, respectively, the membrane, coupling, and flexural rigidities, and Q_{ij} is the laminate transformed reduced stiffnesses.

The governing equations in W and F are derived via the Hu-Washizu mixed formulation for the potential energy[14]:

$$\begin{aligned} \pi = \int_x \int_y \Big\{ \tfrac{1}{2}\Big[& -\{\hat{F} + \bar{N}\}^T[a]\{\hat{F} + \bar{N}\} \\ & + 2\{\hat{F} + \bar{N}\}^T[b]\{\chi\} + \{\chi\}^T[d]\{\chi\} + (F_{,yy} + \bar{N}_{xx})W_{,x}^2 \\ & + (F_{,xx} + \bar{N}_{yy})W_{,y}^2 - 2(F_{,xy} + \bar{N}_{xy})W_{,x}W_{,y} \\ & - 2(F_{,xx} + \bar{N}_{yy})\frac{W}{R(\theta)}\Big] - qW \Big\} dx\, dy \end{aligned} \tag{6}$$

where q is the external applied normal load. Variation of π yields the exact equilibrium and compatibility nonlinear equations.

Employing the perturbation technique (by using the α parameter as the normalized amplitude of the buckling model)

$$\begin{aligned} W &= W^{(0)} + \alpha W^{(1)} \\ F &= F^{(0)} + \alpha F^{(1)} \end{aligned} \tag{7}$$

we obtain the following expression for the potential energy:

$$\pi = \pi^{(0)} + \alpha\pi^{(1)} + \alpha^2\pi^{(2)} \tag{8}$$

The prebuckling equations are derived by setting $\delta\pi^{(1)} = 0$,

$$L_a[W^{(0)}] + L_b[F^{(0)}] + L[F^{(0)}, W^{(0)}] + \bar{N}_{xx} \cdot W_{,xx}^{(0)} + \frac{[F_{,xx}^{(0)} + \bar{N}_{xx}]}{R(\theta)} + q = 0 \tag{9a}$$

$$L_b[W^{(0)}] + L_d[F^{(0)}] + \tfrac{1}{2}L[W^{(0)}, W^{(0)}] + \frac{W_{,xx}^{(0)}}{R(\theta)} = 0 \tag{9b}$$

and the buckling equations by setting $\delta\pi^{(2)} = 0$:

$$L_a[W^{(1)}] + L_b[F^{(1)}] + L[F^{(1)}, W^{(0)}] + L[F^{(0)}, W^{(1)}] + \bar{N}_{xx} \cdot W_{,xx}^{(1)} + \frac{F_{,xx}^{(1)}}{R(\theta)} = 0 \tag{10a}$$

$$L_b[W^{(1)}] + L_d[F^{(1)}] + L[W^{(0)}, W^{(1)}] + \frac{W_{,xx}^{(1)}}{R(\theta)} = 0 \tag{10b}$$

where L and L_p are differential operators defined as

$$\begin{aligned} L(S, T) &= S_{,xx}T_{,yy} - 2S_{,xy}T_{,xy} + S_{,yy}T_{,xx} \\ L_p(S) &= p_{40}S_{,xxxx} + p_{31}S_{,xxxy} + p_{22}S_{,xxyy} + p_{13}S_{,xyyy} + p_{04}S_{,yyyy} \end{aligned} \tag{11}$$

with $p = a$, d, and b. The coefficients a_{ij}, d_{ij}, and b_{ij}, which are expressed in terms of the laminate properties $[a]$, $[b]$, and $[d]$, are given in Ref. 15. Equations (9a) and (10a) refer to the equilibrium and Eqs. (9b) and (10b) to the compatibility. The curvature term $1/R$ is a function of the circumferential coordinate.

The boundary conditions, which are derived in the same manner as in Ref. 16, fall into three distinct groups: simply supported SS_i ($W = M_{xx} = 0$), clamped CC_i ($W = W_{,x} = 0$), and free FF_i ($Q_x^* = M_{xx} = 0$). The subscript $i = 1, \ldots, 4$ denotes the following in-plane conditions: $i = 1$ for $F_{,xy} = F_{,yy} = 0$, $i = 2$ for $F_{,xy} = 0$ and $U = c$, $i = 3$ for $V = F_{,yy} = 0$, and $i = 4$ for $V = 0$ and $U = c$ where c is a constant.

Two noncircular configurations are widely discussed in the literature (see for example Refs. 3, 5, 6, and 11). They are the following:

1) Elliptic, represented by the equation

$$\left(\frac{\bar{y}}{A}\right)^2 + \left(\frac{\bar{z}}{B}\right)^2 = 1 \tag{12}$$

where $\bar{y}$ and $\bar{z}$ are the major and minor coordinates of the ellipse (see Fig. 1), A and B are the half-axes in the $\bar{y}$ and $\bar{z}$ directions, and the circumferential radius of curvature is given by

$$R(y) = \frac{A^2}{B}\left\{1 + \left[\left(\frac{B}{A}\right)^2 - 1\right]\left[\frac{\bar{y}(y)}{A}\right]^2\right\}^{3/2} \tag{13}$$

2) Nonellipsoidal oval, whose radius of curvature is given by

$$R(y) = \frac{R_0}{1 + \xi\cos(2y/R_0)} \tag{14}$$

where ξ is the eccentricity parameter, and R_0 is the radius of a circular cylinder with the same circumference.

Analysis for a noncircular cross section necessitates a general expression for the curvature of any arbitrary configuration. The shape of the cross section can be considered as a periodic function of the circumferential angle (θ) $[R(\theta) = R(\theta + 2\pi)]$ and can be described in terms of a Fourier series. The present study is confined to a cross section with at least two axes of symmetry, thus,

$$\frac{1}{R(\theta)} = \sum_{k=0}^{N} \alpha_k \cos(2k\theta) \tag{15}$$

where θ is the angle coordinate (Fig. 1), and N is the number of terms in the truncated series for the curvature. The curvature of elliptic [Eq. (13)] and oval [Eq. (14)] cross sections can be described exactly by the Fourier series of Eq. (15). (It should be noted here that the oval configuration was considered to simplify the analysis: it is merely an approximate equivalent expression in R_0 and may deviate significantly from the actual cross section.) An example of three configurations with small, medium, and large eccentricity is given in Table 1. In this table the Fourier coefficients of the elliptic shape are for the same major and minor axes length (A and B). The convergence of the Fourier series is shown in Fig. 2 for the medium and large eccentricities.

Since the general Fourier expansion of the curvature [Eq. (15)] is written in terms of the angle θ rather than in that of the circumferential y coordinate, the system equations [Eqs.

(9–11) and boundary conditions] must be transformed from the latter to the former. The transformation is effected through the differential operators L and L_p defined in Eq. (11) as

$$\bar{L}(S, T) = S_{,xx}[rr_{,\theta}T_{,\theta} + r^2T_{,\theta\theta}] - 2[rS_{,\theta}]_{,x}[rT_{,\theta}]_{,x} + [rr_{,\theta}S_{,\theta} + r^2S_{,\theta\theta}]T_{,xx} \tag{16}$$

$$\bar{L}_p(S) = p_{40}S_{,xxxx} + p_{31}[rS_{,\theta}]_{,xxx} + p_{22}[rr_{,\theta}S_{,\theta} + r^2S_{,\theta\theta}]_{,xx} + p_{13}[rr_{,\theta}^2S_{,\theta} + r^2r_{,\theta\theta}S_{,\theta} + 3r^2r_{,\theta}S_{,\theta\theta} + r^3S_{,\theta\theta\theta}]_{,x} + p_{04}[rr_{,\theta}^3S_{,\theta} + 4r^2r_{,\theta}r_{,\theta\theta}S_{,\theta} + r^3r_{,\theta\theta\theta}S_{,\theta} + 7r^2r_{,\theta}^2S_{,\theta\theta} + 4r^3r_{,\theta\theta}S_{,\theta\theta} + 6r^3r_{,\theta}S_{,\theta\theta\theta} + r^4S_{,\theta\theta\theta\theta}]$$

where $r = r(\theta) = 1/R(\theta)$.

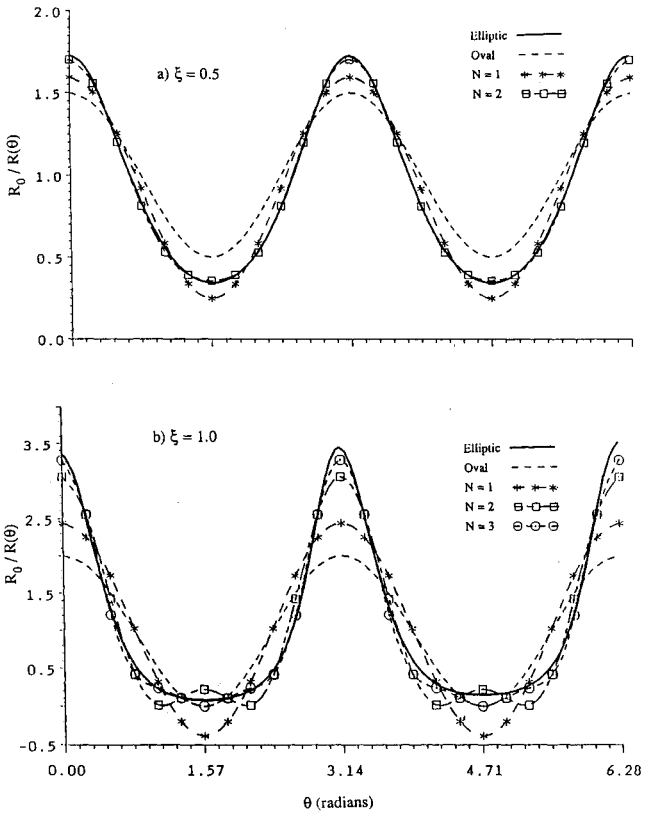

Fig. 2 Curvature of elliptic and oval cross sections in terms of Fourier coefficients: a) $B/A = 0.711$, $\xi = 0.5$ and b) $B/A = 0.485$, $\xi = 1.0$.

III. Solution Methodology

The set of partial differential equations is first reduced to one of ordinary differential equations by separation of variables as

$$W(x, \theta) = \sum_{m=0}^{2N_1} w_m(x)g_m(\theta)$$
$$F(x, \theta) = \sum_{n=0}^{2N_2} f_n(x)g_n(\theta) \tag{17}$$

where N_1 and N_2 are the number of retained terms in the truncated series for W and F, respectively, and

$$g_m(\theta) = \begin{cases} \cos(im\theta) & m = 0,1, \ldots, N_3 \\ \sin(im\theta) & m = N_3 + 1, \ldots, 2N_3 \end{cases} \tag{18}$$

where $N_3 = N_1$ for the W series and $N_3 = N_2$ for the F series, and i denotes the characteristic circumferential wave number. Recourse to a characteristic wave number makes it possible in some cases to reduce substantially the number of terms in the Fourier series.[17] For general cases in which all terms are significant, it is necessary to let $i = 1$ and to let N_1 and N_2 be sufficiently large for an accurate representation of W and F. Applying the Galerkin procedure for minimizing the errors due to the truncated form of the series, the following integrals must vanish:

$$\oint (\text{equilibrium equation})\, g_m^j(\theta)\, d\theta = 0 \qquad j = 0,1, \ldots, 2N_1$$
$$\oint (\text{compatibility equation}) g_n^j(\theta)\, d\theta = 0 \qquad j = 0,1, \ldots, 2N_2 \tag{19}$$

where g_m^j and g_n^j are the weighting functions, chosen as $\cos(ij\theta)$ and $\sin(ij\theta)$. The equilibrium and compatibility equations are Eqs. (9a) and (9b) for the prebuckling state and Eqs. (10a) and (10b) for the buckling state, respectively. With all of the preceding steps implemented, we arrive at the following ordinary differential equations:

Equilibrium:

$$\sum_{m=0}^{2N_1}\Big\{a_{40}A_0(m, p)w_{m,xxxx}^{(e)} + a_{31}A_1(m, p)w_{m,xxx}^{(e)} + [a_{22}A_2(m, p) - \eta\bar{N}_{xx}A_0(m, p)]w_{m,xx}^{(e)} + [a_{13}A_3(m, p) - \eta \cdot 2\bar{N}_{xy}A_1(m, p)]w_{m,x}^{(e)} + [a_{04}A_4(m, p) - \eta\bar{N}_{yy}A_2(m, p)]w_m^{(e)}\Big\} + \sum_{n=0}^{2N_2}\Big\{b_{40}A_0(n, p)f_{n,xxxx}^{(e)} + b_{31}A_1(n, p)f_{n,xxx}^{(e)} + [b_{22}A_2(n, p) + B_1(n, p)]f_{n,xx}^{(e)}$$

Table 1 Nondimensional Fourier expansion of curavature $[R_0/R(\theta)]$ for elliptic and oval cross sections

Eccentricity, ξ	Major axis 2A	Minor axis 2B	Ellipse	Oval
Small = 0.1	2.064	1.932	0.99332 + 0.1111 cos 2θ + 0.00151 cos 4θ	1 + 0.1 cos 2θ
Medium = 0.5	2.298	1.636	0.92058 + 0.67345 cos 2θ + 0.10862 cos 4θ + 0.0129 cos 6θ + 0.00148 cos 8θ	1 + 0.5 cos 2θ
Large = 1.0	2.516	1.22	1.0264 + 1.41091 cos 2θ + 0.60735 cos 4θ + 0.22113 cos 6θ + 0.07684 cos 8θ + 0.02581 cos 10θ	1 + cos 2θ

Table 2 Convergence of buckling load with respect to the truncated N_1 and N_2 for $L/R_0 = 0.7$, CC_1 boundary condition with error up to 1%

	$\xi = 0.1$		$\xi = 0.5$				$\xi = 1.0$					
	$i = 1$	$i = 2$	$i = 1$			$i = 2$	$i = 1$			$i = 2$		
$N_1 = N_2$			sin, cos	sin	cos		sin, cos	sin	cos	sin, cos	sin	cos
1	0.978	1.012	0.809	0.802	1.311	0.848	0.508	0.510	1.597	0.709	1.024	0.709
2	0.983	1.067	0.807	0.792	0.838	0.693	0.509	0.509	0.707	0.334	0.540	0.335
3	1.006	1.073	0.611	0.615	0.875	0.744	0.200	0.202	0.711	0.226	0.314	0.225
4	1.009	1.025	0.616	0.614	1.151	0.578	0.202	0.201	0.334	0.182	0.221	0.179
5	0.951	1.010	0.561	0.558	0.718	0.593	0.150	0.149	0.338	0.176	0.178	0.157
6	0.952	1.014	0.559	0.564	0.628	0.568	0.135	0.150	0.225	0.151	0.157	0.144
7	1.046	1.006	0.543	0.540	0.627	0.572	0.135	0.135	0.241	0.143	0.144	0.131
8	1.030	1.006	0.541	0.546	0.627	0.561	0.129	0.135	0.180	0.136	0.136	0.128
9	0.971	1.006	0.535	0.620	0.643	0.565	0.130	0.130	0.184	0.133	0.132	0.127
10	0.958	1.006	0.535	0.613	0.628	0.565	0.127	0.131	0.170	0.131	0.126	0.127

Table 3 Normalized buckling load for oval cylindrical shell $L/R_0 = 0.7$ ($i = 1$, $N_1 = N_2 = 10$)

ξ	SS_1	SS_2	SS_3	SS_4	CC_1	CC_2	CC_3	CC_4	Ref. 3
0.0	0.529	0.528	1.095	1.086	1.068	1.041	1.093	1.135	1.0
0.1	0.491	0.493	1.050	1.073	0.958	0.949	1.035	1.088	0.918
0.2	0.431	0.432	0.954	0.897	0.862	0.855	0.944	0.946	0.817
0.3	0.380	0.380	0.746	0.762	0.759	0.791	0.846	0.843	0.725
0.4	0.330	0.329	0.632	0.638	0.640	0.728	0.746	0.746	0.630
0.5	0.281	0.280	0.537	0.538	0.536	0.630	0.643	0.645	0.530
0.6	0.229	0.226	0.444	0.451	0.473	0.479	0.523	0.524	0.445
0.7	0.172	0.172	0.343	0.351	0.347	0.349	0.426	0.425	0.345
0.8	0.113	0.113	0.236	0.237	0.238	0.239	0.359	0.357	0.255
0.9	0.064	0.064	0.177	0.180	0.166	0.166	0.228	0.230	0.172
1.0	0.037	0.038	0.051	0.051	0.130	0.130	0.137	0.137	0.105

$$+ b_{13}A_3(n, p)f^{(e)}_{n,x} + b_{04}A_4(n, p)f^{(e)}_n \Big\}$$

$$+ \delta \sum_{m=0}^{2N_1} \sum_{n=0}^{2N_2} \Big\{ C_4(m, n, p)[f^{(0)}_n w^{(1)}_{m,xx} + f^{(1)}_n w^{(0)}_{m,xx}]$$

$$+ C_1(n, m, p)[f^{(0)}_{n,xx} w^{(1)}_m + f^{(1)}_{n,xx} w^{(0)}_m]$$

$$- 2C_2(m, n, p)f^{(e)}_{n,x}[w^{(e)}_{m,x}\Big\} = (1-\delta)2\pi q$$

$$p = 0,1, \ldots, 2N_1 \tag{20}$$

Compatibility:

$$\sum_{m=0}^{2N_1} \Big\{ b_{40}A_0(m, p)w^{(e)}_{m,xxxx} + b_{31}A_1(m, p)w^{(e)}_{m,xxx}$$

$$+ [b_{22}A_2(m, p) + B_1(m, p)]w^{(e)}_{m,xx}$$

$$+ b_{13}A_3(m, p)w^{(e)}_{m,x} + b_{04}A_4(m, p)w^{(e)}_m \Big\}$$

$$+ \sum_{n=0}^{2N_2} \Big\{ d_{40}A_0(n, p)f^{(e)}_{n,xxxx} + d_{31}A_1(n, p)f^{(e)}_{n,xxx}$$

$$+ d_{22}A_2(n, p)f^{(e)}_{n,xx} + d_{13}A_3(n, p)[f^{(e)}_{n,x} + d_{04}A_4(n, p)f^{(e)}_n \Big\}$$

$$+ \delta \sum_{m=0}^{2N_1} \sum_{n=0}^{2N_1} \Big\{ C_1(m, n, p)\Big[w^{(0)}_m w^{(1)}_{n,xx} + w^{(1)}_m w^{(0)}_{n,xx} \Big]$$

$$+ C_2(m,n,p)\Big[w^{(0)}_{m,x} w^{(1)}_{n,x} + w^{(1)}_{m,x} w^{(0)}_{n,x} \Big] \Big\}$$

$$p = 0, 1, \ldots, 2N_2 \tag{21}$$

The superscript e and the multipliers δ indicate the state $e = 0$ and $\delta = 0$ for prebuckling, and e and $\delta = 1$ for buckling; $\eta = 1$ accounts for the nonlinear terms. The solution process consists of two steps: first the prebuckling equations ($e = \delta = 0$) are solved, and the results are substituted in the buckling equations ($e = \delta = 1$), resulting again in a set of ordinary differential equations.

It should be emphasized that the present theory is based on a linear prebuckling behavior, which yields an eigenproblem. The expressions for $A_i(m, p)$, $B_1(m, p)$, and $C_i(m, n, p)$ are given in the Appendix. Actually, these Galerkin coefficients express the equivalent values of the double and triple Fourier series. A special symbolic program using the REDUCE compiler[18] was written for constructing the tables for $A_i(m, p)$, $B_1(m, p)$, and $C_i(m, n, p)$. The boundary conditions of SS_i, CC_i, and FF_i were derived in the same manner and are expressed as functions of the meridional coordinate only (for more details, see Ref. 19). By increasing the number of dependent variables from two (w and f) to four (w, ϕ, f, and φ) where

$$\phi = w_{,xx}$$
$$\varphi = f_{,xx} \tag{22}$$

the sequence is reduced to second order and the number of equations doubled. Finally, the central finite difference scheme is used to reduce the ordinary differential equations to the following algebraic ones:

For the prebuckling state,

$$[K]\{Z\} = \{P\} \tag{23}$$

and for the buckling state,

$$\{[K] + \lambda[G]\}\{Z\} = 0 \tag{24}$$

Table 4 Normalized buckling load for oval cylindrical shell CC_1 ($i = 1$, $N_1 = N_2 = 10$)

	L/R_0		
ξ	0.7	2.0	5.0
0.0	1.068	1.0	1.0
0.1	0.958	1.023	1.059
0.2	0.862	0.963	1.038
0.3	0.759	0.874	0.999
0.4	0.640	0.653	0.933
0.5	0.536	0.548	0.563
0.6	0.473	0.452	0.450
0.7	0.347	0.348	0.349
0.8	0.238	0.286	0.251
0.9	0.166	0.145	0.150
1.0	0.130	0.056	0.052

Table 5 Normalized buckling load of elliptic and oval cross sections ($L/R_0 = 0.7$, CC_1, $i = 1$, $N_1 = N_2 = 10$)

	Elliptic cross section $R_0/R(\theta) = \sum_{k=0}^{N} \alpha_k \cos(2k\theta)$				Oval cross section $R_0/R(\theta) =$
Eccentricity	$N=1$	$N=2$	$N=3$	$N=4$	$1 + \xi \cos 2\theta$
Small $\xi = 0.1$ $B/A = 0.936$	0.941	0.941			0.958
Medium $\xi = 0.5$ $B/A = 0.711$	0.281	0.401	0.387	0.387	0.536
Large $\xi = 1.0$ $B/A = 0.485$	0.186	0.136	0.128	0.135	0.130

where K and G are the stiffness and geometry matrices, respectively; Z is the unknown vector composed of w, ϕ, f, and φ; and λ is the external applied load parameter. Equation (24) is an eigenvalue problem for which λ represents the buckling load parameter and Z the buckling mode.

IV. Numerical Results and Discussion

For the procedure outlined earlier, a general computer program was written, covering the prebuckling and buckling behavior of any laminated cylindrical shell of arbitrary noncircular cross section with two axes of symmetry. The program consists of two parts: 1) a symbolic program for creating the Galerkin coefficients and 2) a Fortran program for the matrix procedure to solve the prebuckling state and the eigenvalue problem for the buckling state. The computer code is applicable for any stacking sequence, accommodates all SS_i, CC_i, and FF_i boundary conditions; and is especially suitable for study of the effect of the eccentricity parameter. The cases of isotropic and laminated noncircular cylindrical shells under axial compression are considered next as examples of parametric study.

Isotropic Shell

The parameters in this example[3] are wavelength, boundary conditions, length-to-radius ratio, and cross-sectional shape. First, convergence of the buckling load with respect to the number of finite difference mesh points and the truncated wave number is checked for the oval configuration. The oval is represented by $R_0/R(\theta) = 1 + \xi \cos 2\theta$ where ξ is the eccentricity parameter of the oval cross section. For 29 mesh points the solution converges with an error of less than 0.1%. As regards convergence with respect to N_1 and N_2, unlike the circular case, there is—because of the high coupling—no single characteristic wave number by which the buckling mode can be represented. Accordingly, two characteristic wave numbers were taken for the check: $i = 1$, which is the most general case whereby all Fourier terms can be included, and $i = 2$, which expresses the coupling between terms with $m - p = 2$ and the curvature. For $i > 2$ the solution did not converge at all since there is no such coupling. It should be clear that $i = 2$ does not include the 2θ coupling of odd wave numbers (5θ–3θ and so on). Consequently, it is recommended to assign the characteristic wave number $i = 1$ and take N_1 and N_2 as large as possible for the solution to converge with a given error. The procedure is summarized in Table 2 for small ($\xi = 0.1$), medium ($\xi = 0.5$), and large ($\xi = 1.0$) eccentricity. In addition, the symmetric (cosine) and asymmetric (sine) modes were considered separately so as to bring out the coupling effect. The buckling loads were normalized as $N_{xx} = Eh^2/[R\sqrt{3(1-\nu^2)}]$. The normalized buckling loads for SS_i and CC_i boundary conditions vs the results of Ref. 3 are given in Table 3 which refer to long shells in which the boundary conditions are irrelevant. The effect of the length-to-radius ratio on the buckling load is shown in Table 4. Finally, the elliptic cross section is considered through expansion of the curvature in the θ coordinate (see Table 1). The results vs the oval cross section are listed in Table 5. It seems that for small and large eccentricity the ellipse buckles under almost the same axial load as the oval, whereas for medium eccentricity the buckling load of the elliptic cross section is significantly lower. The reason is that in the former case the two cross sections have almost the same minimum curvature at which buckling sets in; in the latter case the minimum curvature of the ellipse is significantly lower than that of the oval. This also accounts for the direction of convergence with respect to N (truncated term of curvature). For example, the curvature for the medium eccentricity with $N = 1$ is the lowest, whereas that with $N = 2$ is highest in representing the elliptic configuration (see Fig. 2).

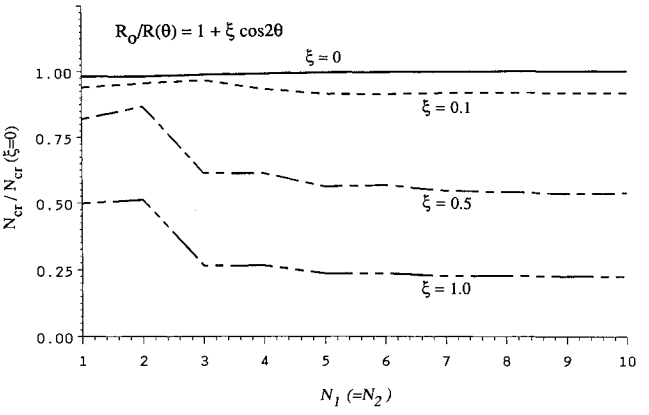

Fig. 3 Convergence with respect to the truncated wave number for layup ± 30 deg.

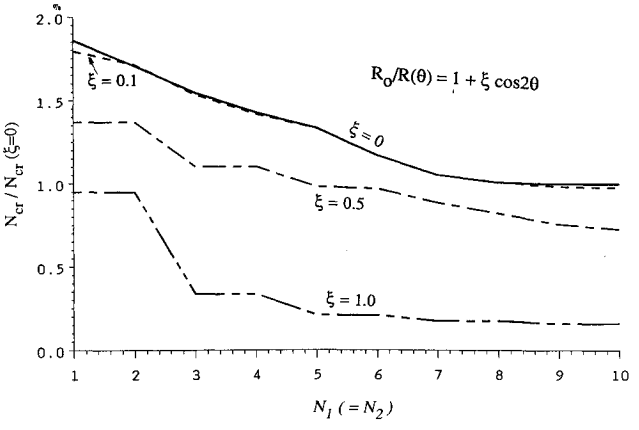

Fig. 4 Convergence with respect to the truncated wave number for layup 90/60/30/0 deg.

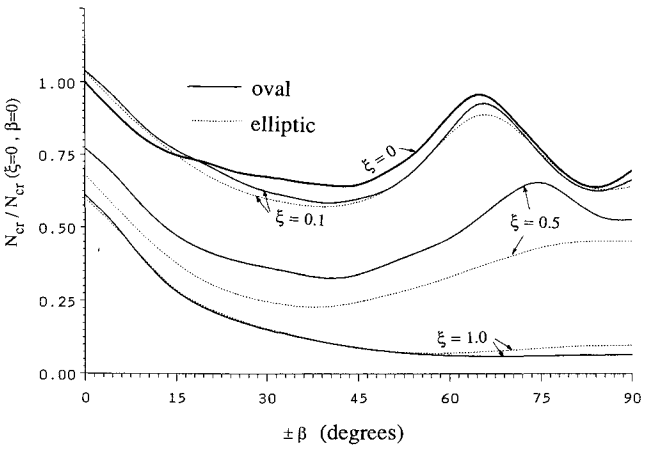

Fig. 5 Buckling load vs orientation angle for elliptic and oval cross sections ($i = 1$, $N_1 = N_2 = 10$).

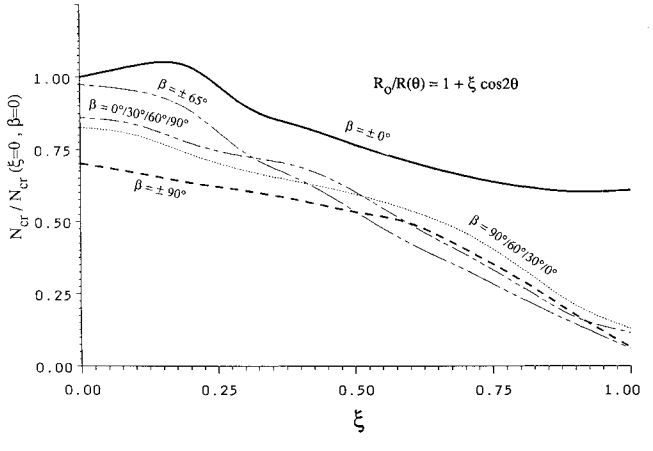

Fig. 6 Buckling load vs oval eccentricity for some stacking combinations ($i = 1$, $N_1 = N_2 = 10$).

Laminated Shell

This example deals with a graphite/epoxy noncircular cylindrical shell with data $E_{11} = 14 \times 10^{10}$ N/m^2; $E_{22} = 0.97 \times 10^{10}$ N/m^2; $G_{12} = 0.41 \times 10^{10}$ N/m^2, $\nu_{12} = 0.26$, $L/R_0 = 0.7$, $R_0/h = 100$, and CC_1 boundary condition. Two laminate layups, angle-ply and 90/60/30/0 deg, are considered (the 90-deg layup is the outer ply). Convergence of the buckling load with respect to the number of mesh points was again obtained for 29 points to an error of 0.1%. Convergence with respect to the truncated wave number for the two layups is shown in Figs. 3 and 4, respectively. The buckling loads are plotted in Fig. 5 vs the orientation angle β. It is seen that for medium eccentricity the difference between the two configurations is the largest, again because the smallest curvature of the elliptic cross section is significantly less than that of the oval one for $\xi = 0.5$ (see Fig. 2). The effect of oval eccentricity is plotted in Fig. 6 for different layups.

V. Conclusion

A buckling analysis and a solution procedure are presented for laminated cylindrical shells with arbitrary noncircular cross sections. The general procedure, achieved through Fourier expansion of the curvature, provides a highly efficient tool for parametric study of the noncircularity parameter. Unlike the circular cylindrical shell, the coupling of the wave number becomes very significant, especially as the shape eccentricity increases. Thus, all wave number terms must be taken for accurate results. From the results presented earlier it is clear that the simple oval expression cannot represent any noncircular cross section, not even the elliptic configuration at certain eccentricities. With the real configuration expanded in Fourier series, the accurate buckling load can be obtained. The present algorithm can be used as a guideline for nonlinear behavior and as a basic procedure for extension to nonlinear analysis in the future.

Appendix: Galerkin Coefficients

Define

$$\frac{1}{R(\theta)} = \sum_{k=0}^{N} \alpha_k r_k(\theta)$$

$$r_k(\theta) = \cos(2k\theta)$$

and let $(\cdot)$ denote the derivative with respect to the θ coordinate:

$$A_0(m, p) = \oint g_m g_p \, d\theta$$

$$A_1(m, p) = \oint \sum_k \alpha_k r_k \dot{g}_m g_p \, d\theta$$

$$A_2(m, p) = \oint \sum_{k1} \sum_{k2} \alpha_{k1}\alpha_{k2}(r_{k1}\dot{r}_{k2}\dot{g}_m + r_{k1}r_{k2}\ddot{g}_m)g_p \, d\theta$$

$$A_3(m, p) = \oint \sum_{k1} \sum_{k2} \sum_{k3} \alpha_{k1}\alpha_{k2}\alpha_{k3}(r_{k1}\dot{r}_{k2}\dot{r}_{k3}\dot{g}_m + r_{k1}r_{k2}\ddot{r}_{k3}\dot{g}_m + 3r_{k1}r_{k2}\dot{r}_{k3}\ddot{g}_m + r_{k1}r_{k2}r_{k3}\dddot{g}_m)g_p \, d\theta$$

$$A_4(m, p) = \oint \sum_{k1} \sum_{k2} \sum_{k3} \sum_{k4} \alpha_{k1}\alpha_{k2}\alpha_{k3}\alpha_{k4}(r_{k1}\dot{r}_{k2}\dot{r}_{k3}\dot{r}_{k4}\dot{g}_m + 4r_{k1}r_{k2}\dot{r}_{k3}\ddot{r}_{k4}\dot{g}_m + r_{k1}r_{k2}r_{k3}\dddot{r}_{k4}\dot{g}_m + 7r_{k1}r_{k2}\dot{r}_{k3}\dot{r}_{k4}\ddot{g}_m + 4r_{k1}r_{k2}r_{k3}\ddot{r}_{k4}\ddot{g}_m + 6r_{k1}r_{k2}r_{k3}\dot{r}_{k4}\dddot{g}_m + r_{k1}r_{k2}r_{k3}r_{k4}\ddddot{g}_m)g_p \, d\theta$$

$$B_1(m, p) = \oint \sum_k \alpha_k r_k g_m g_p \, d\theta$$

$$C_1(m, n, p) = \oint \sum_{k1} \sum_{k2} \alpha_{k1}\alpha_{k2}(r_{k1}\dot{r}_{k2}\dot{g}_m + r_{k1}r_{k2}\ddot{g}_m)g_n g_p \, d\theta$$

$$C_2(m, n, p) = \oint \sum_{k1} \sum_{k2} \alpha_{k1}\alpha_{k2} r_{k1}r_{k2}\dot{g}_m\dot{g}_n g_p \, d\theta$$

Acknowledgments

The study was financed in part by the VPR Foundation of the Technion. The authors are indebted to E. Goldberg for editorial assistance.

References

[1]Simitses, G. J., "Buckling and Postbuckling of Imperfect Cylindrical Shells: A Review," *Applied Mechanics Reviews*, Vol. 39, No. 10, 1986, pp. 1517–1524.

[2]Volpe, V., Chen, Y. N., and Kempner, J., "Buckling of Orthogonality Stiffened Finite Oval Cylindrical Shells Under Axial Compression and Lateral Pressure," Dept. of Mechanical Engineering, Polytechnic Inst. of New York, Poly-M/AE Rept. 78-10, Troy, New York, 1978.

[3]Volpe, V., Chen, Y. N., and Kempner, J., "Buckling of Orthogonally Stiffened Finite Oval Cylindrical Shells Under Axial Compression," *AIAA Journal*, Vol. 18, No. 5, 1980, pp. 571–580.

[4]Kempner, J., and Chen, Y. N., "Large Deflections of an Axially Compressed Oval Cylindrical Shell," *Proceedings of the Eleventh International Congress of Applied Mechanics* (Munich), Springer-Verlag, Berlin, Germany, 1964, pp. 299–306.

[5]Kempner, J., and Chen, Y. N., "Buckling and Postbuckling of an Axially Compressed Oval Cylindrical Shell," *Proceedings of the Symposium on the Theory of Shells to Honor Lloyd H. Donnell*, McCuthan Pub. Co., 1967, pp. 141–183.

[6]Hutchinson, J. W., "Buckling and Initial Post-Buckling Behavior of Oval Cylindrical Shells Under Axial Compression," *ASME Journal of Applied Mechanics*, Vol. 35, No. 1, 1968, pp. 66–72.

[7]Feinstein, G., Erickson, B., and Kempner, J., "Stability of Oval Cylindrical Shells," *Journal of Experimental Mechanics*, Vol. 11, No. 11, 1971, pp. 514–520.

[8]Feinstein, G., Chen, Y. N., and Kempner, J. "Buckling of Clamped Oval Cylindrical Shells Under Axial Loads," *AIAA Journal*, Vol. 9, No. 9, 1971, pp. 1733–1738.

[9]Chen, Y. N., and Kempner, J., "Buckling of Oval Cylindrical Shells Under Compression and Asymmetric Bending," *AIAA Journal*, Vol. 14, No. 9, 1976, pp. 1235–1240.

[10]Soldatos, K. P., and Tzivanidis, G. J., "Buckling and Vibration of Cross-Ply Laminated Non-Circular Cylindrical Shells," *Journal of Sound and Vibration*, Vol. 82, No. 32, 1982, pp. 425–434.

[11]Sun, G., "Buckling and Initial Post-Buckling Behavior of Laminated Oval Cylindrical Shells Under Axial Compression," *ASME Journal of Applied Mechanics*, Vol. 58, No. 9, 1991, pp. 848–851.

[12]Koumousis, V. K., and Armenakas, A. E., "Free Vibrations of Simply Supported Cylindrical Shells of Oval Cross-Section," *AIAA Journal*, Vol. 21, No. 7, 1983, pp. 1017–1027.

[13]Soldatos, K. P., "A Flugge-Type Theory for the Analysis of Anisotropic Laminated Non-Circular Cylindrical Shells," *International Journal of Solids and Structures*, Vol. 20, No. 2, 1984, pp. 107–120.

[14]Sheinman, I., and Reichman, Y., "A Study of Buckling and Vibration of Laminated Shallow Curved Panels," *International Journal of Solids and Structures*, Vol. 29, No. 11, 1992, pp. 1329–1338.

[15]Sheinman, I., Frostig, Y., and Segal, A., "Bifurcation Buckling Analysis of Stiffened Laminated Composite Panels," *Buckling of Structures*, edited by I. Elishakoff, J. Arbocz, C. D. Babcook, Jr., and A. Libai, Elsevier Science Publisher, Amsterdam, The Netherlands, 1988, pp. 355–380.

[16]Sheinman, I., and Simitses, G. J., "Buckling Analysis of Geometrically Imperfect Stiffened Cylinders Under Axial Compression," *AIAA Journal*, Vol. 15, No. 3, 1977, pp. 374–382.

[17]Narasimhan, K. Y., and Hoff, N. D., "Calculation of the Load Carrying Capacity of Initially Slightly Imperfect Thin Walled Circular Cylindrical Shells of Finite Length," Stanford Univ., Dept. of Aeronautics and Astronautics, SUDAER No. 329, Stanford, CA, 1967.

[18]Hearn, A. C., "REDUCE—User's Manual, Version 3.2," Rand Corporation, CP78, Santa Monica, CA, July 1987.

[19]Firer, M., "Dynamic Stability of Non-Circular Laminated Cylindrical Shells," Ph.D. Thesis, Faculty of Civil Engineering, Technion—Israel Institute of Technology, Haifa, Israel, 1993.